

Chapter 15

Analytical Models for Multihop Cognitive Radio Networks

Yi Shi and Y. Thomas Hou

Contents

15.1	Introduction	383
15.2	Analytical Models at Multiple Layers	386
15.2.1	Modeling of Available Spectrum Allocation	386
15.2.2	Modeling of Power Control and Scheduling	388
15.2.3	Flow Routing and Link Capacity Model	392
15.3	Case Study	393
15.3.1	Case A: Subband Division and Allocation Problem	394
15.3.2	Case B: Power Control Problem	398
15.4	Conclusion	404
	Acknowledgment	405
	References	405

15.1 Introduction

A cognitive radio (CR) is a frequency-agile data communication device with a rich control and monitoring (spectrum sensing) interface [11]. It capitalizes on advances in signal processing and radio technology, as well as recent changes in spectrum policy. A CR node constantly senses the spectrum to detect any change in white space; its frequency-agile radio module is

capable of reconfiguring RF and switching to newly-selected frequency bands. A CR can be programmed to tune to a wide spectrum range and operate on any frequency band in the range.

The need for CR functionality is indeed compelling, as it affects many important wireless communications applications, including public safety, military, and wireless applications for the general public. Since its conceptual inception, there has been growing interest in the research community to develop cognitive radio platforms. As research in CR continues to intensify, it is expected that future truly CR networks will ultimately have the processing power and flexibility needed to support spectrum sensing, flexible waveform configuration, spectrum negotiation in dynamic environments, and many other functions. Also, it is not hard to foresee that CR will eventually play a pivotal role in multihop wireless networking, such as mesh and ad hoc networks, which are currently mostly based on 802.11 technology. Under CR-enabled wireless networks, each node individually detects the white bands at its particular location, and the spectrum that can be used for communication can be different from node to node. It is not unusual to find that although each node may have some white bands to access, there still may not exist a common frequency band shared by all the nodes in the network.

To better understand the unique challenges associated with a CR-enabled wireless network, we compare it with multichannel multiradio (MC-MR) wireless networks (e.g., [1, 7, 14]), which have been an area of active research in recent years. First, an MC-MR platform employs traditional *hardware-based* radio technology (i.e., channel coding, modulation, etc. are all implemented in hardware). Thus, each radio can only operate on a single channel at a time and there is no switching of channels on a per-packet basis. The number of concurrent channels that can be used at a wireless node is limited by the number of hardware-based radios. In contrast, the radio technology in CR is software-based; a CR is capable of switching frequency bands on a per-packet basis and over a wide range of spectrum. As a result, the number of concurrent frequency bands that can be shared by a single CR is typically much larger than what can be supported by MC-MR. Second, due to the nature of hardware-based radio technology in MC-MR, a common assumption in MC-MR is that there is a set of *common* channels available for every node in the network; each channel typically has the same bandwidth. Such an assumption may not hold for CR networks, in which each node may have a different set of frequency bands, each of potentially unequal size. A CR node is capable of working on a set of “heterogeneous” channels that are scattered across widely separated slices of the frequency spectrum with different bandwidths. An even more profound advance in CR technology is that there is no requirement that a CR needs to select contiguous frequencies/channels for transmission/reception—the radio can send packets over noncontiguous frequency bands. These important differences

between MC-MR and CR warrant that the algorithm design for a CR network be substantially more complex than that under MC-MR. In some sense, an MC-MR-based wireless network can be considered as a special (simple) case of a CR-based wireless network. Thus, algorithms designed for a CR network can be tailored to address MC-MR networks while *the converse is not true*.

Due to the unique characteristics associated with CR networks, problems for CR networks are expected to be much more challenging and interesting. As a first step toward studying CR networks systematically, it is important to develop analytical models. Such models should capture characteristics of CR across multiple layers, such as power control, scheduling, and routing. Performance objectives should correlate with spectrum usage and its occupancy in space, which are unique to CR networks. The goal of this chapter is to present a unified mathematical model for the physical (i.e., power control), link (i.e., scheduling), and network (i.e., routing) layers in a multihop cognitive radio network environment.

The foundation of our analytical model is built upon the so-called interference modeling. There are two popular approaches to model interference in wireless networks, namely, the *physical model* and the *protocol model*. Under the *physical model* (see, e.g., [3,5,6,8,10]), a transmission is considered successful if and only if the signal-to-interference-and-noise ratio (SINR) exceeds a certain threshold, where the interference includes all other concurrent transmissions. Since the calculation of a link's capacity involves not only the transmission power on this link, but also the transmission power on interference links, it is difficult to develop a tractable optimal solution whenever link capacity is involved. Another approach to model interference is called the *protocol model* [10], whereby a transmission is considered successful if and only if the receiving node is in the transmission range of the corresponding transmission node and is out of the interference range of all other transmission nodes. This model is easy to understand and facilitates the building of tractable models. It has been used successfully to address various hard problems in wireless networks (see, e.g., [1,4,13–15,19]); results from these efforts have already offered many important insights. In this chapter, we will follow the protocol model in our analytical modeling.

We organize this chapter as follows. In Section 15.2, we present an analytical model for a multihop CR network at multiple layers. Within this section, we start in Section 15.2.1 with the modeling problem of spectrum band division and allocation, which is unique to CR networks. Then in Section 15.2.2, based on the protocol interference model, we develop an analytical model in the form of a set of constraints for power control and scheduling. Finally, in Section 15.2.3, we present models for flow routing and link capacity. To show the application of the mathematical models in Section 15.2, we apply these models to solving some real problems for

multihop CR networks in Section 15.3. We first present a new objective function called the *bandwidth footprint product* (BFP), which uniquely characterizes the spectrum and space occupancy for a node in a CR network. Using this objective function, we study two specific problems in a multihop CR network. In Section 15.3.1, we study the subband division and allocation problem under fixed transmission power (i.e., no power control). The goal is to explore how the different-sized available bandwidth in the network should be optimally divided and allocated among the nodes. In Section 15.3.2, we study the power control problem when all the subbands are identical (i.e., fixed channel bandwidth). The goal there is to explore how to optimally adjust the power level for each node in the network so that the total BFP is minimized. The results from these two case studies not only validate the practical utility of the analytical models, but also help gain some theoretical understanding of a multihop CR network.

15.2 Analytical Models at Multiple Layers

We consider an ad hoc network consisting of a set of \mathcal{N} nodes. Among these nodes, there is a set of \mathcal{L} unicast communication sessions. Denote $s(l)$ and $d(l)$ the source and destination nodes of session $l \in \mathcal{L}$, and $r(l)$ the rate requirement (in b/s) of session l . Table 15.1 lists all notation used in this chapter.

15.2.1 Modeling of Available Spectrum Allocation

This part of mathematical modeling is unique to CR networks and does not exist in MC-MR networks. In a multihop CR network, the available spectrum bands at one node may be different from those at another node in the network. Given a set of available frequency bands at a node, the sizes (or bandwidths) of each band may differ drastically. For example, among the least-utilized spectrum bands found in [17], the bandwidth between [1240, 1300] MHz (allocated to amateur radio) is 60 MHz, while the bandwidth between [1525, 1710] MHz (allocated to mobile satellites, GPS systems, and meteorological applications) is 185 MHz. Such large differences in bandwidths among the available bands suggests the need for further division of the larger bands into smaller subbands for more flexible and efficient frequency allocation. Since equal subband division of the available spectrum band is likely to yield suboptimal performance, an unequal division is desirable.

More formally, we model the union of the available spectrum among all the nodes in the network as a set of M unequally sized bands (see Figure 15.1). \mathcal{M} denotes the set of these bands and $\mathcal{M}_i \subseteq \mathcal{M}$ denotes the set of available bands at node $i \in \mathcal{N}$, which is possibly different from that at another node, say $j \in \mathcal{N}$, i.e., $\mathcal{M}_i \neq \mathcal{M}_j$. For example, at node i ,

Table 15.1 Notation

Symbol	Definition
d_{ij}	Distance between nodes i and j
$d(l)$	Destination node of session l
$f_{ij}(l)$	Data rate that is attributed to session l on link (i, j)
g_{ij}	Propagation gain from node i to node j
h_{ij}^m	$\in \{0, 1, 2, \dots, H\}$, the integer power level for q_{ij}^m
H	The total number of power levels at a transmitter
\mathcal{T}_j^m	The set of nodes that can use band m and are within the interference range of node j
$K^{(m)}$	The maximum number for subband division in band m
\mathcal{L}	The set of active user sessions in the network
\mathcal{M}_i	The set of available bands at node $i \in \mathcal{N}$
\mathcal{M}	$= \bigcup_{i \in \mathcal{N}} \mathcal{M}_i$, the set of available bands in the network
M	$= \mathcal{M} $, the number of available bands in the network
\mathcal{M}_{ij}	$= \mathcal{M}_i \cap \mathcal{M}_j$, the set of available bands on link (i, j)
n	Path loss index
\mathcal{N}	The set of nodes in the network
$q_{ij}^{(m,k)}$	The transmission power spectral density from node i to node j in subband (m, k)
Q	Maximum transmission power spectral density at a transmitter
Q_T	The minimum threshold of power spectral density to decode a transmission at a receiver
Q_I	The maximum threshold of power spectral density for interference to be negligible at a receiver
$r(l)$	Rate of session $l \in \mathcal{L}$
$R_T(q), R_I(q)$	Transmission range and interference range under q , respectively
R_T^{\max}, R_I^{\max}	Transmission range and interference range under Q , respectively
$s(l)$	Source node of session l
\mathcal{T}_i^m	The set of nodes that can use band m and are within the transmission range of node i
\mathcal{T}_i	$= \bigcup_{m \in \mathcal{M}} \mathcal{T}_i^m$, the set of nodes within the transmission range of node i
$u^{(m,k)}$	The fraction of bandwidth for the k -th subband in band m
$W^{(m)}$	Bandwidth of band $m \in \mathcal{M}$
$x_{ij}^{(m,k)}$	Binary indicator to mark whether or not subband (m, k) is used by link (i, j) .
β	An antenna-related constant
η	Ambient Gaussian noise density

\mathcal{M}_i may consist of bands I, III, and V, while at node j , \mathcal{M}_j may consist of bands I, IV, and VI. $W^{(m)}$ denotes the bandwidth of band $m \in \mathcal{M}$. For more flexible and efficient bandwidth allocation and to overcome the disparity in bandwidth size among the spectrum bands, we assume that band m can be

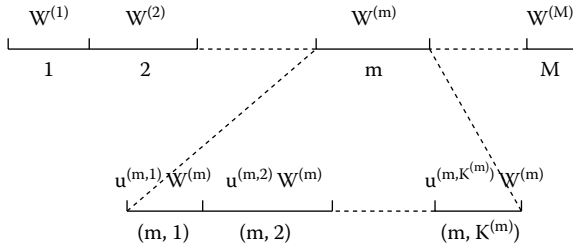


Figure 15.1 A schematic illustrating the concept of bands and subbands in spectrum sharing.

further divided into up to $K^{(m)}$ subbands, each of which may be of *unequal* bandwidth. $u^{(m,k)}$ denotes the fraction of bandwidth for the k -th subband in band m . Then we have

$$\sum_{k=1}^{K^{(m)}} u^{(m,k)} = 1.$$

As an example, Figure 15.1 shows M bands in the network and for a specific band m , it displays a further division into $K^{(m)}$ subbands. Then the M bands in the network are effectively divided into $\sum_{m=1}^M K^{(m)}$ subbands, each of which may be of different size. Note that for a specific optimization problem, some $u^{(m,k)}$ s can be 0 in the final optimal solution. This suggests that we will have fewer subbands than $K^{(m)}$ in the optimal solution.

15.2.2 Modeling of Power Control and Scheduling

In this section, we show analytical models for power control and scheduling for multihop CR networks. We will examine the notion of transmission and interference ranges in a wireless network, as well as the necessary and sufficient condition for successful transmission.

Transmission and Interference Ranges. We follow the protocol model for a wireless network [10], where each transmitting node is associated with a transmission range and an interference range. Both transmission and interference ranges directly depend on a node’s transmission power and propagation gain. For transmission from node i to node j , a widely used model for power propagation gain g_{ij} is

$$g_{ij} = \beta d_{ij}^{-n}, \tag{15.1}$$

where β is an antenna-related constant, d_{ij} is the physical distance between nodes i and j , and n is the path loss index. Note that we are considering

a uniform gain model here and assuming the same gain model on all frequency bands. The case of a nonuniform gain model or a band-dependent gain behavior can be extended without much technical difficulty.

In this context, we assume a data transmission from node i to node j is successful only if the received power spectral density at node j exceeds a threshold, say Q_T . Suppose node i 's transmission power spectral density is q and denote the transmission range of this node as $R_T(q)$. Then based on $g_{ij} \cdot q \geq Q_T$ and (15.1), we can calculate the transmission range of this node as follows:

$$R_T(q) = \left(\frac{q}{Q_T} \right)^{1/n}. \quad (15.2)$$

Similarly, we assume that an interference is non-negligible only if it exceeds a power spectral density threshold, say Q_I , at a receiver. Denote the interference range of a node by $R_I(q)$. Then following the same reasoning as in the derivation for the transmission range, we can obtain the interference range of a node as follows:

$$R_I(q) = \left(\frac{q}{Q_I} \right)^{1/n}.$$

Note that since $Q_I < Q_T$, the interference range is greater than the transmission range at a node, i.e., $R_I(q) > R_T(q)$.

Necessary and Sufficient Condition for Successful Transmission. In a CR network, each node has a set of frequency subbands that it may use for transmission and reception. Suppose that subband (m, k) is available at both node i and node j , and $q_{ij}^{(m,k)}$ denotes the transmission power from node i to node j in subband (m, k) . Then to schedule a successful transmission from node i to node j , the following necessary and sufficient condition, expressed as two constraints, must be met. The first constraint (C-1) is that receiving node j must be physically within the transmission range of node i , i.e.,

$$(C-1) \quad d_{ij} \leq R_T(q_{ij}^{(m,k)}) = \left(\frac{q_{ij}^{(m,k)}}{Q_T} \right)^{1/n}.$$

The second constraint (C-2) is that the receiving node j must not fall into the interference range of any other node p ($p \in \mathcal{N}$, $p \neq i$) that is transmitting on the same subband, i.e.,

$$(C-2) \quad d_{jp} \geq R_I(q_{pz}^{(m,k)}) = \left(\frac{q_{pz}^{(m,k)}}{Q_I} \right)^{1/n},$$

where z is the intended receiving node of transmitting node p .

Now we formalize the necessary and sufficient condition for successful transmission into a mathematical model in the general context of multihop CR networks. Suppose that subband (m, k) is available at both node i and node j , i.e., $m \in \mathcal{M}_{ij}$, where $\mathcal{M}_{ij} = \mathcal{M}_i \cap \mathcal{M}_j$. Define

$$x_{ij}^{(m,k)} = \begin{cases} 1 & \text{if node } i \text{ transmits data to node } j \text{ on subband } (m, k), \\ 0 & \text{otherwise.} \end{cases}$$

We consider scheduling in the frequency domain. Thus, once a subband (m, k) is used by node i for transmission to node j , $m \in \mathcal{M}_{ij}$, this subband cannot be used again by node i to transmit to a different node. That is,

$$(C-3) \quad \sum_{j \in T_i^m} x_{ij}^{(m,k)} \leq 1,$$

where T_i^m is the set of nodes that are within the transmission range of node i under full power spectral density Q on band m .

R_T^{\max} denotes the maximum transmission range of a node when it transmits at full power. Then based on (15.2), we have

$$R_T^{\max} = R_T(Q) = \left(\frac{Q}{Q_T} \right)^{1/n}.$$

Thus, we have

$$Q_T = \frac{Q}{(R_T^{\max})^n}.$$

Then for a node transmitting at a power $q \in [0, Q]$, its transmission range is

$$R_T(q) = \left(\frac{q}{Q_T} \right)^{1/n} = \left[\frac{q(R_T^{\max})^n}{Q} \right]^{1/n} = \left(\frac{q}{Q} \right)^{1/n} R_T^{\max}. \quad (15.3)$$

Similarly, R_I^{\max} denotes the maximum interference range of a node when it transmits at full power. Then by the same token we have

$$R_I^{\max} = R_I(Q) = \left(\frac{Q}{Q_I} \right)^{1/n},$$

$$Q_I = \frac{Q}{(R_I^{\max})^n}.$$

For a node transmitting at a power $q \in [0, Q]$, its interference range is

$$R_I(q) = \left(\frac{q}{Q}\right)^{1/n} R_I^{\max}. \quad (15.4)$$

Recall that \mathcal{T}_i^m denotes the set of nodes that are within the transmission range from node i under full power spectral density Q on band m . More formally, we have $\mathcal{T}_i^m = \{j : d_{ij} \leq R_T^{\max}, j \neq i, m \in \mathcal{M}_j\}$. Similarly, \mathcal{I}_j^m denotes the set of nodes that can cause interference to node j on band m under full power spectral density Q , i.e., $\mathcal{I}_j^m = \{p : d_{jp} \leq R_I^{\max}, m \in \mathcal{M}_p\}$. Note that the definitions of \mathcal{T}_i^m and \mathcal{I}_j^m are both based on full transmission power spectral density Q . When the power spectral density level q is below Q , the corresponding transmission and interference ranges will be smaller. As a result, it is necessary to keep track of the set of nodes that fall into the transmission range and the set of nodes that can produce interference whenever transmission power changes at a node.

Applying (15.3) and (15.4) to the two constraints (C-1) and (C-2) for successful transmission from node i to node j , we have

$$d_{ij} \leq R_T(q_{ij}^{(m,k)}) = \left(\frac{q_{ij}^{(m,k)}}{Q}\right)^{1/n} R_T^{\max}, \quad (15.5)$$

$$d_{jp} \geq R_I(q_{pz}^{(m,k)}) = \left(\frac{q_{pz}^{(m,k)}}{Q}\right)^{1/n} R_I^{\max} \quad (p \in \mathcal{I}_j^m, p \neq i, z \in \mathcal{T}_p^m). \quad (15.6)$$

Based on (15.5) and (15.6), we have the following requirements for the transmission link $i \rightarrow j$ and interfering link $p \rightarrow z$:

$$q_{ij}^{(m,k)} \begin{cases} \in \left[\left(\frac{d_{ij}}{R_T^{\max}}\right)^n Q, Q \right] & \text{if } x_{ij}^{(m,k)} = 1, \\ = 0 & \text{if } x_{ij}^{(m,k)} = 0, \end{cases}$$

$$q_{pz}^{(m,k)} \leq \begin{cases} \left(\frac{d_{pj}}{R_I^{\max}}\right)^n Q & \text{if } x_{ij}^{(m,k)} = 1, \\ Q & \text{if } x_{ij}^{(m,k)} = 0, \end{cases} \quad (p \in \mathcal{I}_j^m, p \neq i, z \in \mathcal{T}_p^m).$$

Mathematically, these requirements can be rewritten as

$$(C-1') \quad q_{ij}^{(m,k)} \in \left[\left(\frac{d_{ij}}{R_T^{\max}}\right)^n Q x_{ij}^{(m,k)}, Q x_{ij}^{(m,k)} \right],$$

$$(C-2') \quad q_{pz}^{(m,k)} \leq Q - \left[1 - \left(\frac{d_{pj}}{R_I^{\max}}\right)^n \right] Q x_{ij}^{(m,k)} \quad (p \in \mathcal{I}_j^m, p \neq i, z \in \mathcal{T}_p^m).$$

Recall that we consider scheduling in the frequency domain, and that in (C-3) we state that once a subband (m, k) is used by node i for transmission to node j , this subband cannot be used again by node i to transmit to a different node. In addition, for successful scheduling in the frequency domain, the following two constraints must also hold:

- (C-4) For a subband (m, k) that is available at node j , this subband cannot be used for both transmission and receiving. That is, if subband (m, k) is used at node j for transmission (or receiving), then it cannot be used for receiving (or transmission).
- (C-5) Similarly to constraint (C-3) on transmission, node j cannot use the same subband (m, k) for receiving from two different nodes.

Note that (C-4) can be viewed as a “self-interference” avoidance constraint where at the same node j , its transmission to another node z on band m interferes with its reception from node i on the same band. It turns out that the above two constraints are mathematically *embedded* in (C-1') and (C-2'). That is, once (C-1') and (C-2') are satisfied, then both constraints (C-4) and (C-5) are also satisfied. This result is formally stated in the following lemma. Its proof can be found in [20].

Lemma 15.1

If transmission powers on every transmission link and interference link satisfy (C-1') and (C-2') in the network, then (C-4) and (C-5) are also satisfied.

The significance of Lemma 15.1 is that since (C-4) and (C-5) are embedded in (C-1') and (C-2'), they can be removed from the list of scheduling constraints. That is, it is sufficient to consider constraints (C-1'), (C-2'), and (C-3) for scheduling and power control.

15.2.3 Flow Routing and Link Capacity Model

Recall that we consider an ad hoc network consisting of a set of \mathcal{N} nodes. Among these nodes, there is a set of \mathcal{L} active user communication (unicast) sessions. $s(l)$ and $d(l)$ denote the source and destination nodes of session $l \in \mathcal{L}$ and $r(l)$ denotes the rate requirement (in b/s) of session l . To route these flows from their respective source nodes to their destination nodes, it is necessary to employ multihop due to limited transmission range of a node. Further, to have better load balancing and flexibility, it is desirable to employ multipath routing (i.e., allow flow splitting) between a source node and its destination node. This is because a single path is overly restrictive and usually does not yield an optimal solution.

Mathematically, this can be modeled as follows. $f_{ij}(l)$ denotes the data rate on link (i, j) that is attributed to session l , where $i \in \mathcal{N}$,

$j \in \mathcal{T}_i = \bigcup_{m \in \mathcal{M}_i} \mathcal{T}_i^m$. If node i is the source node of session l , i.e., $i = s(l)$, then

$$\sum_{j \in \mathcal{T}_i} f_{ij}(l) = r(l). \quad (15.7)$$

If node i is an intermediate relay node for session l , i.e., $i \neq s(l)$ and $i \neq d(l)$, then

$$\sum_{j \in \mathcal{T}_i}^{j \neq s(l)} f_{ij}(l) = \sum_{k \in \mathcal{T}_i}^{k \neq d(l)} f_{ki}(l). \quad (15.8)$$

If node i is the destination node of session l , i.e., $i = d(l)$, then

$$\sum_{k \in \mathcal{T}_i} f_{ki}(l) = r(l). \quad (15.9)$$

It can be easily verified that once (15.7) and (15.8) are satisfied, (15.9) must also be satisfied. As a result, it is sufficient to have (15.7) and (15.8) in the formulation.

In addition to the above flow balance equations at each node $i \in \mathcal{N}$ for session $l \in \mathcal{L}$, the aggregated flow rates on each radio link cannot exceed this link's capacity. Under $q_{ij}^{(m,k)}$, we have

$$\begin{aligned} \sum_{l \in \mathcal{L}}^{s(l) \neq j, d(l) \neq i} f_{ij}(l) &\leq \sum_{m \in \mathcal{M}_{ij}} \sum_{k=1}^{K^{(m)}} c_{ij}^{(m,k)} \\ &= \sum_{m \in \mathcal{M}_{ij}} \sum_{k=1}^{K^{(m)}} W^{(m)} u^{(m,k)} \log_2 \left(1 + \frac{g_{ij}}{\eta W} q_{ij}^{(m,k)} \right), \end{aligned} \quad (15.10)$$

where η is the ambient Gaussian noise density. Note that the denominator inside the log function contains only ηW . This is due to the use of protocol interference modeling, i.e., when node i is transmitting to node j on band m , then the interference range of all other nodes on this band should not contain node j .

15.3 Case Study

In the last section, we presented analytical models for power control, scheduling, and flow routing. In this section, we show how to apply these analytical models to solve some real problems for multihop CR networks.

First and foremost, we should have an objective function. For CR networks, a number of objective functions can be considered for problem

formulation. A commonly used objective is to maximize network capacity, which can be expressed as maximizing a scaling factor for all the rate requirements of the communication sessions in the network (see, e.g., [1, 14]). For CR networks, we consider an objective called the bandwidth footprint product (BFP), which characterizes the spectrum and space occupancy for the nodes in a CR network. The BFP was first introduced by Liu and Wang in [16]. The so-called footprint refers to the interference area of a node under a given transmission power, i.e., $\pi \cdot (R_I(q))^2$. Since each node in the network will use a number of bands for transmission and each band will have a certain footprint corresponding to its transmission power, an important objective is to minimize the network-wide BFP, which is the sum of BFPs among all the nodes in the network. That is, our objective is to minimize

$$\sum_{i \in \mathcal{N}} \sum_{m \in \mathcal{M}_i} \sum_{j \in \mathcal{T}_i^m} \sum_{k=1}^{K^{(m)}} W^{(m)} u^{(m,k)} \cdot \pi (R_I(q_{ij}^{(m,k)}))^2,$$

which is equal to

$$\pi (R_I^{\max})^2 \sum_{i \in \mathcal{N}} \sum_{m \in \mathcal{M}_i} \sum_{j \in \mathcal{T}_i^m} \sum_{k=1}^{K^{(m)}} W^{(m)} u^{(m,k)} \left(\frac{q_{ij}^{(m,k)}}{Q} \right)^{2/n}.$$

Since $\pi (R_I^{\max})^2$ is a constant factor, we can remove it from the objective function.

Using this objective function, we study two specific problems for CR networks. In Section 15.3.1, we study the subband division and allocation problem under fixed transmission power (i.e., no power control). The goal is to explore how the different-sized available bandwidth in the network should be optimally divided and allocated among the nodes. In Section 15.3.2, we study the power control problem when all the subbands are identical (i.e., fixed channel bandwidth). The goal there is to explore how to optimally adjust the power level at each node in the network so that the objective function is minimized.

15.3.1 Case A: Subband Division and Allocation Problem

Problem Formulation. In this case study, we focus on subband division and spectrum sharing for CR networks. We assume the transmission power spectral density is Q and is fixed, i.e.,

$$q_{ij}^{(m,k)} = \begin{cases} Q & \text{if } x_{ij}^{(m,k)} = 1, \\ 0 & \text{if } x_{ij}^{(m,k)} = 0, \end{cases}$$

which is equivalent to

$$q_{ij}^{(m,k)} = Qx_{ij}^{(m,k)}. \tag{15.11}$$

As a result, the objective function of minimizing the network-wide BFP is equivalent to minimizing the network-wide bandwidth usage, i.e., $\sum_{i \in \mathcal{N}} \sum_{m \in \mathcal{M}_i} \sum_{j \in \mathcal{T}_i^m} \sum_{k=1}^{K^{(m)}} Wu^{(m,k)}(x_{ij}^{(m,k)})^{2/n}$. Since $x_{ij}^{(m,k)}$ is a binary variable (0 or 1), this is equivalent to minimizing

$$\sum_{i \in \mathcal{N}} \sum_{m \in \mathcal{M}_i} \sum_{j \in \mathcal{T}_i^m} \sum_{k=1}^{K^{(m)}} Wu^{(m,k)} x_{ij}^{(m,k)}.$$

We now examine the power control and scheduling constraints (C-1') and (C-2') under fixed transmission power. Due to (15.11), (C-1') always holds and thus can be removed from problem formulation. Due to fixed transmission power, (C-2') can be rewritten as

$$Qx_{pz}^{(m,k)} \leq Q - \left[1 - \left(\frac{d_{pj}}{R_I^{\max}} \right)^n \right] Qx_{ij}^{(m,k)} \quad (p \in \mathcal{T}_j^m, p \neq i, z \in \mathcal{T}_p^m),$$

which is equal to

$$x_{pz}^{(m,k)} \begin{cases} = 0 & \text{if } x_{ij}^{(m,k)} = 1. \\ \leq 1 & \text{if } x_{ij}^{(m,k)} = 0 \end{cases} \quad (p \in \mathcal{T}_j^m, p \neq i, z \in \mathcal{T}_p^m),$$

since $x_{pz}^{(m,k)}$ and $x_{ij}^{(m,k)}$ are binary variables. Thus, $x_{pz}^{(m,k)} + x_{ij}^{(m,k)} \leq 1$ for $p \in \mathcal{T}_j^m, p \neq i, z \in \mathcal{T}_p^m$. On the other hand, $\sum_{z \in \mathcal{T}_p^m} x_{pz}^{(m,k)} \leq 1$ due to (C-3). Putting these together into a more compact form, we have

$$\sum_{z \in \mathcal{T}_p^m} x_{pz}^{(m,k)} + x_{ij}^{(m,k)} \leq 1 \quad (p \in \mathcal{T}_j^m, p \neq i).$$

Under fixed transmission power, the link capacity constraint (15.10) is

$$\sum_{l \in \mathcal{L}}^{s(l) \neq j, d(l) \neq i} f_{ij}(l) \leq \sum_{m \in \mathcal{M}_{ij}} \sum_{k=1}^{K^{(m)}} W^{(m)} u^{(m,k)} \log_2 \left(1 + \frac{g_{ij} Q}{\eta W} \right) x_{ij}^{(m,k)}.$$

Now we have the following optimization problem for subband division and allocation:

$$\text{Min} \quad \sum_{i \in \mathcal{N}} \sum_{m \in \mathcal{M}_i} \sum_{j \in \mathcal{T}_i^m} \sum_{k=1}^{K^{(m)}} W^{(m)} x_{ij}^{(m,k)} u^{(m,k)}$$

$$\text{s.t.} \quad \sum_{k=1}^{K^{(m)}} u^{(m,k)} = 1 \quad (m \in \mathcal{M}),$$

$$\sum_{j \in \mathcal{T}_i^m} x_{ij}^{(m,k)} \leq 1 \quad (i \in \mathcal{N}, m \in \mathcal{M}_i, 1 \leq k \leq K^{(m)}),$$

$$x_{ij}^{(m,k)} + \sum_{z \in \mathcal{T}_p^m} x_{pz}^{(m,k)} \leq 1 \quad (i \in \mathcal{N}, m \in \mathcal{M}_i, j \in \mathcal{T}_i^m,$$

$$1 \leq k \leq K^{(m)}, p \in \mathcal{T}_j^m, p \neq i),$$

$$\sum_{l \in \mathcal{L}}^{s(l) \neq j, d(l) \neq i} f_{ij}(l) - \sum_{m \in \mathcal{M}_i} \sum_{k=1}^{K^{(m)}} W^{(m)} \log_2 \left(1 + \frac{g_{ij} Q}{\eta} \right) x_{ij}^{(m,k)} u^{(m,k)}$$

$$\leq 0 \quad (i \in \mathcal{N}, j \in \mathcal{T}_i),$$

$$\sum_{j \in \mathcal{T}_i} f_{ij}(l) = r(l) \quad (l \in \mathcal{L}, i = s(l)),$$

$$\sum_{j \in \mathcal{T}_i}^{j \neq s(l)} f_{ij}(l) - \sum_{p \in \mathcal{T}_i}^{p \neq d(l)} f_{pi}(l) = 0 \quad (l \in \mathcal{L}, i \in \mathcal{N}, i \neq s(l), d(l)),$$

$$x_{ij}^{(m,k)} = 0 \text{ or } 1, u^{(m,k)} \geq 0 \quad (i \in \mathcal{N}, m \in \mathcal{M}_i, j \in \mathcal{T}_i^m, 1 \leq k \leq K^{(m)}),$$

$$f_{ij}(l) \geq 0 \quad (l \in \mathcal{L}, i \in \mathcal{N}, i \neq d(l), j \in \mathcal{T}_i, j \neq s(l)),$$

where $W^{(m)}, g_{ij}, Q, \eta,$ and $r(l)$ are constants, while $x_{ij}^{(m,k)}, u^{(m,k)},$ and $f_{ij}(l)$ are optimization variables.

The above optimization problem is a *mixed-integer nonlinear programming* (MINLP) problem, which is NP-hard in general [9]. Although existing software (e.g., BARON [2]) can solve very small-sized network instances (e.g., several nodes), the time complexity becomes prohibitively high for large-sized networks.

Solution Approach. Here we show a promising approach to solving this problem. Under this approach, we first find a lower bound for the objective via a linear relaxation, which is done by relaxing the integer

variables and using a linearization technique. Using this lower bound as a performance benchmark, we develop a highly effective algorithm based on a so-called *sequential fixing* (SF) procedure [12]. The main idea of SF is to determine the binary variables in the scheduling decisions iteratively via the relaxed formulation. Specifically, since the integer variables $x_{ij}^{(m,k)}$ can only have binary values of either 0 or 1, we can set $x_{ij}^{(m,k)}$ iteratively based on their closeness to either 0 or 1 in the solution to the relaxed formulation. That is, if during an iteration $x_{ij}^{(m,k)}$ has a value close to 1, then we can make a scheduling decision by fixing this $x_{ij}^{(m,k)}$ to 1. In the next iteration, by updating the relaxed problem with these newly fixed values, we can continue the same process to determine (fix) other $x_{ij}^{(m,k)}$ variables. The iteration continues until we fix all the $x_{ij}^{(m,k)}$ s to binary values. The details of this approach can be found in [12].

Simulation Results. The performance of the SF algorithm can be substantiated by simulation results. Specifically, we will show that the solution obtained via the SF algorithm is very close to the lower bound. Since the optimal objective value lies between the lower bound and the solution obtained by the SF algorithm, the solution given by the SF algorithm must be even closer to the true optimum.

We consider $|\mathcal{N}| = 20$ nodes in a 500×500 area (in meters). Among these nodes, there are $|\mathcal{L}| = 5$ active sessions, each with a random rate within $[10, 100]$ Mb/s. We assume that there are $M = 5$ bands that can be used for the entire network (see Table 15.2). Recall that the set of available bands at each CR node is a *subset* of these five bands depending on the node's location, and the sets of available bands at any two nodes in the network may not be identical. In the simulation, this aspect is modeled by randomly selecting a subset of bands from the pool of five bands for each node. Further, we assume that bands I to V can be divided into 3, 5, 2, 4, and 4 subbands, although other desirable divisions can be used. Note that the size of each subband may be unequal and is part of the optimization problem. We assume that the transmission range at each node is 100 m and that the interference range is 150 m. The path loss index n is assumed to be 4, and $\beta = 62.5$. The threshold Q_T is assumed to be

Table 15.2 Available Bands \mathcal{M} in the Network in the Simulation Study

Band Index	Spectrum Range (MHz)	Bandwidth (MHz)
I	[1240, 1300]	60.0
II	[1525, 1710]	185.0
III	[902, 928]	26.0
IV	[2400, 2483.5]	83.5
V	[5725, 5850]	125.0

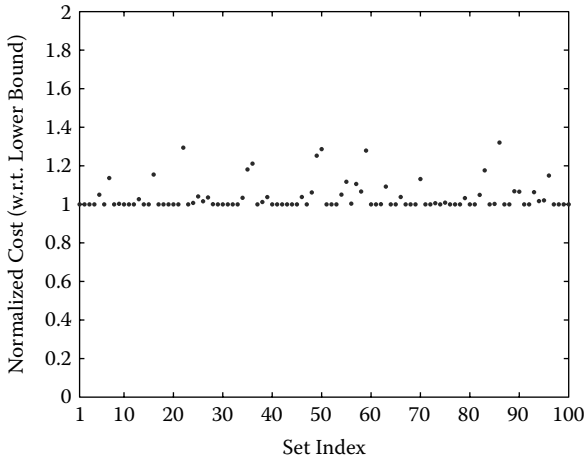


Figure 15.2 Normalized costs (with respect to lower bound) on 100 sets of randomly generated 20-node networks.

10η . Thus, we have $Q_I = \left(\frac{100}{150}\right)^n Q_T$ and the transmission power spectral density $Q = (100)^n Q_T / \beta = 1.6 \cdot 10^7 \eta$.

We present simulation results for 100 randomly generated data sets for 20-node networks. Figure 15.2 shows the normalized costs for 100 data sets. The running time for each point is less than 10 seconds on a Pentium 3.4 GHz machine. For each point, we use the SF algorithm to determine the cost, which is the total required bandwidth in the objective function. Then we normalize this cost with respect to the lower bound obtained by linear relaxation. The average normalized cost among the 100 simulations is 1.04 and the standard deviation is 0.07. There are two observations that can be made from this figure. First, since the ratio of the solution obtained by SF (upper bound of optimal solution) to the lower bound solution is close to 1 (in many cases, they coincide with each other), the lower bound must be very tight. Second, since the optimal solution (unknown) is between the solution obtained by the SF algorithm and the lower bound, *the SF solution must be even closer to the optimum*.

15.3.2 Case B: Power Control Problem

Problem Formulation. In this case study, we focus on power control for CR networks. We assume that \mathcal{M} bands are divided equally, each with a bandwidth W . The set of available bands at each node i is \mathcal{M}_i .

For power control, we allow the transmission power spectral density to be adjusted between 0 and Q . In practice, the transmission power spectral

density can only be tuned into a finite number of discrete levels between 0 and Q . To model this discrete version of power control, we introduce an integer parameter H that represents the total number of power levels to which a transmitter can be adjusted, i.e., $0, \frac{1}{H}Q, \frac{2}{H}Q, \dots, Q$. Denote $b_{ij}^m \in \{0, 1, 2, \dots, H\}$ the integer power level for q_{ij}^m , i.e., $q_{ij}^m = \frac{b_{ij}^m}{H}Q$.

Under such discrete levels of power control, constraints (C-1'), (C-2'), and (15.10) can be rewritten as follows:

$$b_{ij}^m \in \left[\left(\frac{d_{ij}}{R_I^{\max}} \right)^n Hx_{ij}^m, Hx_{ij}^m \right], \tag{15.12}$$

$$b_{pz}^m \leq H - \left[1 - \left(\frac{d_{pj}}{R_I^{\max}} \right)^n \right] Hx_{ij}^m \quad (p \in \mathcal{I}_j^m, p \neq i, z \in \mathcal{T}_p^m), \tag{15.13}$$

$$\sum_{l \in \mathcal{L}}^{s(l) \neq j, d(l) \neq i} f_{ij}(l) \leq \sum_{m \in \mathcal{M}_{ij}} W \log_2 \left(1 + \frac{g_{ij}Q}{\eta WH} b_{ij}^m \right).$$

For the objective function, again we consider the bandwidth footprint product (BFP), which is

$$\begin{aligned} & \pi(R_I^{\max})^2 \sum_{i \in \mathcal{N}} \sum_{m \in \mathcal{M}_i} \sum_{j \in \mathcal{T}_i^m} W \left(\frac{q_{ij}^m}{Q} \right)^{2/n} \\ &= \pi(R_I^{\max})^2 \sum_{i \in \mathcal{N}} \sum_{m \in \mathcal{M}_i} \sum_{j \in \mathcal{T}_i^m} W \left(\frac{b_{ij}^m}{H} \right)^{2/n}. \end{aligned}$$

Since $\pi(R_I^{\max})^2$ is a constant factor, we can remove it from the objective function.

Putting all these together, we have the following formulation:

$$\text{Min} \quad \sum_{i \in \mathcal{N}} \sum_{m \in \mathcal{M}_i} \sum_{j \in \mathcal{T}_i^m} W \left(\frac{b_{ij}^m}{H} \right)^{2/n}$$

$$\text{s.t.} \quad \sum_{j \in \mathcal{T}_i^m} x_{ij}^m \leq 1 \quad (i \in \mathcal{N}, m \in \mathcal{M}_i),$$

$$b_{ij}^m - \left(\frac{d_{ij}}{R_I^{\max}} \right)^n Hx_{ij}^m \geq 0 \quad (i \in \mathcal{N}, m \in \mathcal{M}_i, j \in \mathcal{T}_i^m), \tag{15.14}$$

$$b_{ij}^m - Hx_{ij}^m \leq 0 \quad (i \in \mathcal{N}, m \in \mathcal{M}_i, j \in \mathcal{T}_i^m), \tag{15.15}$$

$$\sum_{z \in \mathcal{T}_p^m} b_{pz}^m + \left(1 - \left(\frac{d_{pj}}{R_i^{\max}}\right)^n\right) Hx_{ij}^m \leq H$$

$$(i \in \mathcal{N}, m \in \mathcal{M}_i, j \in \mathcal{T}_i^m, p \in \mathcal{T}_j^m, p \neq i), \quad (15.16)$$

$$\sum_{l \in \mathcal{L}}^{s(l) \neq j, d(l) \neq i} f_{ij}(l) - \sum_{m \in \mathcal{M}_{ij}} W \log_2 \left(1 + \frac{g_{ij} Q}{\eta WH} b_{ij}^m\right) \leq 0, \quad (i \in \mathcal{N}, j \in \mathcal{T}_i)$$

$$\sum_{j \in \mathcal{T}_i} f_{ij}(l) = r(l) \quad (l \in \mathcal{L}, i = s(l)),$$

$$\sum_{j \in \mathcal{T}_i}^{j \neq s(l)} f_{ij}(l) - \sum_{p \in \mathcal{T}_i}^{p \neq d(l)} f_{pi}(l) = 0 \quad (l \in \mathcal{L}, i \in \mathcal{N}, i \neq s(l), d(l)),$$

$$x_{ij}^m \in \{0, 1\}, b_{ij}^m \in \{0, 1, 2, \dots, Q\} \quad (i \in \mathcal{N}, m \in \mathcal{M}_i, j \in \mathcal{T}_i^m),$$

$$f_{ij}(l) \geq 0 \quad (l \in \mathcal{L}, i \in \mathcal{N}, i \neq d(l), j \in \mathcal{T}_i, j \neq s(l)),$$

where $W, g_{ij}, R_T^{\max}, R_I^{\max}, Q, \eta, r(l)$, and H are constants, and x_{ij}^m, b_{ij}^m , and $f_{ij}(l)$ are optimization variables. In this formulation, (15.14) and (15.15) come from (15.12), while (15.16) is based on (15.13) by noting that in (C-3) there is at most one $z \in \mathcal{T}_p^m$ such that $x_{pz}^m = 1$. As a result, by (15.15) there is at most one $z \in \mathcal{T}_p^m$ such that $b_{pz}^m > 0$. Thus, (15.13) can be rewritten as

$$\sum_{z \in \mathcal{T}_p^m} b_{pz}^m \leq H - \left(1 - \left(\frac{d_{pi}}{R_i^{\max}}\right)^n\right) Hx_{ij}^m \quad (p \in \mathcal{T}_j^m, p \neq i),$$

which is equivalent to (15.16).

This optimization problem is in the form of a *mixed-integer nonlinear programming* (MINLP) problem, which is NP-hard in general [9]. In [20], we developed a solution procedure based on branch-and-bound approach [18] and convex hull relaxation. The details of this solution approach are quite mathematically involved, and we refer readers to [20].

Simulation Results. To offer some insights into the power control problem, we present some simulation results from [20]. We consider a 20-node ad hoc network with each node randomly placed in a 500×500 area (in meters). An instance of network topology is given in Figure 15.3 with each node's location listed in Table 15.3. We assume there are $|\mathcal{M}| = 10$ frequency bands in the network and each band has a bandwidth of

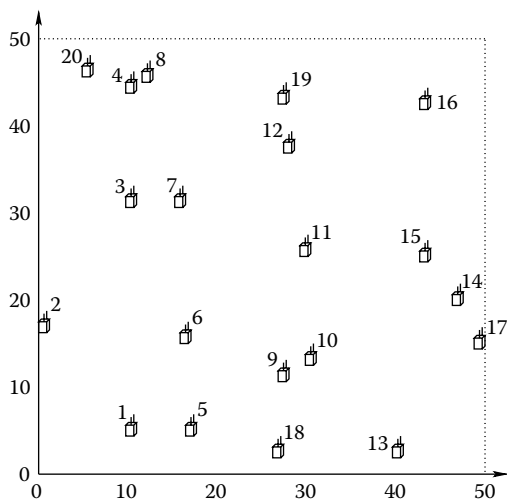


Figure 15.3 A 20-node ad hoc network.

Table 15.3 Each Node's Location and Available Frequency Bands for the 20-node Network

Node Index	Location	Available Bands
1	(10.5, 4.3)	I, II, III, IV, V, VI, VII, VIII, IX, X
2	(1.7, 17.3)	II, III, IV, V, VI, VII, X
3	(10.7, 30.8)	I, III, IV, V, VI, VII, VIII, IX, X
4	(10.2, 45.3)	I, III, IV, V, VI, VII, VIII, IX, X
5	(17.8, 4)	I, II, V, VI, VII, VIII, IX
6	(17.2, 15.2)	I, II, IV, VIII
7	(16.9, 30.8)	I, II, III, IV, V, VI, VII, VIII, IX, X
8	(12.3, 47.3)	I, III, IV, V, VII, VIII, IX
9	(28.2, 11.5)	I, III, V, VII
10	(32.1, 13.8)	I, II, III, IV, VI, VII, VIII, IX, X
11	(30.4, 25.6)	I, II, III, V, VI, VIII, IX, X
12	(29.7, 36)	I, II, III, IV, VI, VI
13	(41.7, 3.1)	I, II, III, V, VI, VIII, IX, X
14	(41.7, 3.1)	I, IV, V, VIII, IX, X
15	(43.3, 25.3)	II, III, IV, V, VI, VII, VIII, IX, X
16	(44.1, 42.7)	I, II, IV, VI, VII, VIII, IX, X
17	(49.6, 15.8)	I, II, III, IV, V, VI, VII, VIII
18	(28.7, 2.5)	I, II, III, VI, VII, VIII, IX, X
19	(28, 43.5)	II, IV, V, VI, VIII
20	(5, 46.9)	II, IV, V, VI, VII

Table 15.4 Source Node, Destination Node, and Rate Requirement of the Five Active Sessions

Source Node	Destination Node	Rate Requirement
7	16	28
8	5	12
15	13	56
2	18	75
9	11	29

$W = 50$ MHz. Each node may only have a subset of these frequency bands. In the simulation, this is modeled by randomly selecting a subset of bands for each node from the pool of 10 bands. Table 15.3 shows the available bands for each node.

We assume that, under maximum transmission power, the transmission range of each node is 100 m and the interference range is twice the transmission range (i.e., 200 m). Both transmission range and interference range will be smaller when transmission power is less than maximum. The path loss index n is assumed to be 4, and $\beta = 62.5$. The threshold Q_T is assumed to be 10η . Thus, we have $Q_I = \left(\frac{100}{200}\right)^n Q_T$ and the maximum transmission power spectral density $Q = (100)^n Q_T / \beta = 1.6 \cdot 10^7 \eta$.

Within the network, we assume there are $|\mathcal{L}| = 5$ user communication sessions, with source node and destination node randomly selected and the rate of each session randomly generated within $[10, 100]$. Table 15.4 specifies an instance of the source node, destination node, and rate requirement for the 5 sessions in the network.

We apply the solution procedure to the 20-node network described above for different levels of power control granularity (H). Under the branch-and-bound solution procedure we set the desired approximation error bound ε to be 0.05, which guarantees that the obtained solution is within 5% of the optimum [20].

Note that $H = 1$ corresponds to the case that there is no power control, i.e., a node uses its peak power spectral density Q for transmission. When H is sufficiently large, the discrete nature of power control diminishes and power control becomes continuous between $[0, Q]$.

Figure 15.4 shows the results of our solution procedure. First, we note that power control has a significant impact on BFP. Comparing the case when there is no power control ($H = 1$) and the case of $H = 15$, we find that there is nearly a 40% reduction in the total cost (objective value). Second, the cost (objective) is a nonincreasing function of H . However, when H becomes sufficiently large (e.g., 10 in this network setting), further increases in H will not yield much reduction in cost. This suggests that for practical purposes, the number of power levels to achieve a reasonably good result does not need to be a large number.

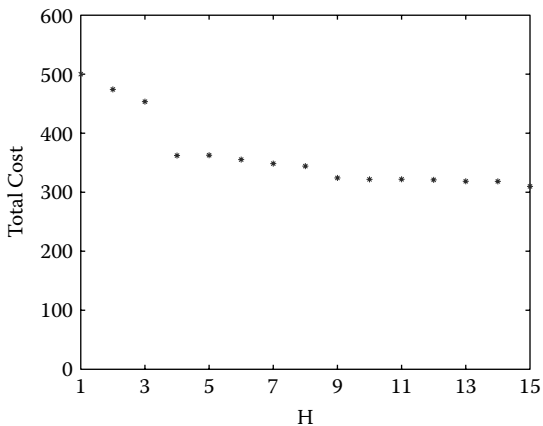


Figure 15.4 Total cost as a function of the number of power levels.

For $H = 10$, the transmission power levels are

$$b_{9,11}^1 = 3,$$

$$b_{12,16}^2 = 4,$$

$$b_{7,12}^3 = 3,$$

$$b_{2,1}^4 = 4,$$

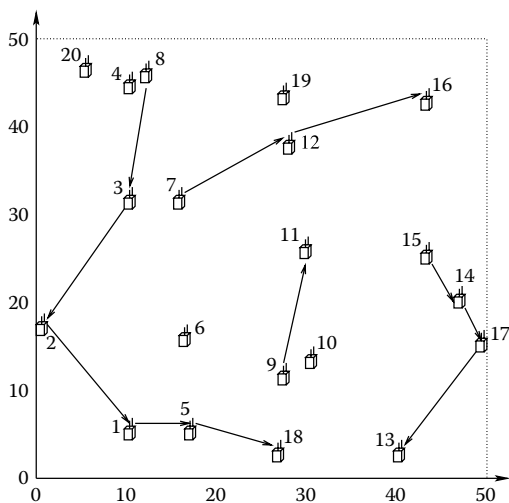


Figure 15.5 Flow routing topology for the five communication sessions in the 20-node network ($H = 10$).

$$\begin{aligned}
b_{2,1}^5 &= 4, \\
b_{5,18}^6 &= 2, \\
b_{17,13}^7 &= 4, \\
b_{8,3}^8 &= 5, \quad b_{14,17}^8 = 1, \\
b_{1,5}^9 &= 1, \quad b_{15,14}^9 = 1, \\
b_{3,2}^{10} &= 5.
\end{aligned}$$

For each $b_{ij}^m > 0$, the corresponding scheduling variable $x_{ij}^m = 1$, otherwise $x_{ij}^m = 0$. The flow routing topology for $H = 10$ is shown in Figure 15.5. The corresponding flow rates are:

$$\begin{aligned}
f_{7,12}(1) &= 28, \quad f_{12,16}(1) = 28, \\
f_{8,3}(2) &= 12, \quad f_{3,2}(2) = 12, \quad f_{2,1}(2) = 12, \quad f_{1,5}(2) = 12, \\
f_{15,14}(3) &= 56, \quad f_{14,17}(3) = 56, \quad f_{17,13}(3) = 56, \\
f_{2,1}(4) &= 75, \quad f_{1,5}(4) = 75, \quad f_{5,18}(4) = 75, \\
f_{9,11}(5) &= 29.
\end{aligned}$$

Note that a link may be used by multiple sessions. For example, link (2, 1) is used by sessions 2 and 4. As a result, the total data rate on link (2, 1) is $f_{2,1}(2) + f_{2,1}(4) = 12 + 75 = 87$.

15.4 Conclusion

Cognitive radio (CR) is a revolution in radio technology that promises unprecedented flexibility in radio communications and is viewed as an enabling technology for future wireless networks. Due to the unique characteristics associated with CR networks, problems for CR networks are expected to be much more challenging and interesting. In this chapter, we presented an analytical model for a multihop CR network at multiple layers. The basic building block in our analytical model is the protocol interference model. Building upon this protocol model, we presented models for power control, scheduling, and routing at physical, link, and network layers, respectively. To demonstrate the practical utility of these analytical models, we studied two practical problems in a multihop CR network as case studies. The first case study addressed the subband division and allocation problem, and the second addressed the power control problem. The results from these two case studies not only validated the practical utility of the analytical models, but also helped gain some theoretical understanding of a multihop CR network.

Acknowledgment

This work has been supported in part by NSF Grant CNS-0721570 and ONR Grant N00014-05-0481.

References

- [1] M. Alicherry, R. Bhatia, and L. Li, "Joint channel assignment and routing for throughput optimization in multi-radio wireless mesh networks," in *Proc. ACM Mobicom*, pp. 58–72, Cologne, Germany, Aug. 28–Sep. 2, 2005.
- [2] BARON Global Optimization Software, <http://www.andrew.cmu.edu/user/ns1b/baron/baron.html>.
- [3] A. Behzad and I. Rubin, "Impact of power control on the performance of ad hoc wireless networks," in *Proc. IEEE Infocom*, pp. 102–113, Miami, FL, March 13–17, 2005.
- [4] R. Bhatia and M. Kodialam, "On power efficient communication over multi-hop wireless networks: joint routing, scheduling and power control," in *Proc. IEEE Infocom*, pp. 1457–1466, Hong Kong, China, March 7–11, 2004.
- [5] C.C. Chen and D.S. Lee, "A joint design of distributed QoS scheduling and power control for wireless networks," in *Proc. IEEE Infocom*, Barcelona, Catalunya, Spain, April 23–29, 2006.
- [6] R.L. Cruz and A.V. Santhanam, "Optimal routing, link scheduling and power control in multi-hop wireless networks," in *Proc. IEEE Infocom*, pp. 702–711, San Francisco, CA, March 30–April 3, 2003.
- [7] R. Draves, J. Padhye, and B. Zill, "Routing in multi-radio, multi-hop wireless mesh networks," in *Proc. ACM Mobicom*, pp. 114–128, Philadelphia, PA, Sep. 26–Oct. 1, 2004.
- [8] T. Elbatt and A. Ephremides, "Joint scheduling and power control for wireless ad hoc networks," in *Proc. IEEE Infocom*, pp. 976–984, New York, NY, June 23–27, 2002.
- [9] M.R. Garey and D.S. Johnson, *Computers and Intractability: A Guide to the Theory of NP-completeness*, W.H. Freeman and Company, pp. 245–248, New York, NY, 1979.
- [10] P. Gupta and P.R. Kumar, "The capacity of wireless networks," *IEEE Transactions on Information Theory*, vol. 46, no. 2, pp. 388–404, March 2000.
- [11] S. Haykin, "Cognitive radio: Brain-empowered wireless communications," *IEEE Journal on Selected Areas in Communications*, vol. 23, no. 2, pp. 201–220, Feb. 2005.
- [12] Y.T. Hou, Y. Shi, and H.D. Sherali, "Optimal spectrum sharing for multi-hop software defined radio networks," in *Proc. IEEE Infocom*, pp. 1–9, Anchorage, AL, May 6–12, 2007.
- [13] K. Jain, J. Padhye, V. Padmanabhan, and L. Qiu, "Impact of interference on multi-hop wireless network performance," in *Proc. ACM Mobicom*, pp. 66–80, San Diego, CA, Sep. 14–19, 2003.

- [14] M. Kodialam and T. Nandagopal, "Characterizing the capacity region in multi-radio multi-channel wireless mesh networks," in *Proc. ACM Mobicom*, pp. 73–87, Cologne, Germany, Aug. 28–Sep. 2, 2005.
- [15] P. Kyasanur and N.H. Vaidya, "Capacity of multi-channel wireless networks: impact of number of channels and interfaces," in *Proc. ACM Mobicom*, pp. 43–57, Cologne, Germany, Aug. 28–Sep. 2, 2005.
- [16] X. Liu and W. Wang, "On the characteristics of spectrum-agile communication networks," in *Proc. IEEE DySpan*, pp. 214–223, Baltimore, MD, Nov. 8–11, 2005.
- [17] M. McHenry and D. McCloskey, "New York City Spectrum Occupancy Measurements September 2004," available at http://www.sharedspectrum.com/inc/content/measurements/nsf/NYC_report.pdf.
- [18] G.L. Nemhauser and L.A. Wolsey, *Integer and Combinatorial Optimization*, John Wiley & Sons, New York, NY, 1999.
- [19] K. Ramachandran, E. Belding-Royer, K. Almeroth, and M. Buddhikot, "Interference-aware channel assignment in multi-radio wireless mesh networks," in *Proc. IEEE Infocom*, Barcelona, Spain, April 23–29, 2006.
- [20] Y. Shi and Y.T. Hou, "Optimal power control for multi-hop software defined radio networks," in *Proc. IEEE Infocom*, pp. 1694–1702, Anchorage, AL, May 6–12, 2007.